Chemical Adaptor Immunotherapy: Design, Synthesis, and Evaluation of Novel Integrin-Targeting Devices

Lian-Sheng Li, Christoph Rader,† Masayuki Matsushita, Sanjib Das, Carlos F. Barbas, III, Richard A. Lerner,* and Subhash C. Sinha*

The Skaggs Institute for Chemical Biology and Department of Molecular Biology, The Scripps Research Institute, 10550 North Torrey Pines Road, La Jolla, California 92037

Received May 4, 2004

A series of β-diketone derivatives of RGD peptidomimetics that selectively bind to $\alpha v\beta 3$ and $\alpha v\beta 5$ integrins were synthesized and covalently docked to the reactive lysine residues of monoclonal aldolase antibody 38C2. The resulting targeting devices strongly and selectively bound to human cancer cells expressing integrins $\alpha v\beta 3$ and $\alpha v\beta 5$ as analyzed by flow cytometry. In vitro and in vivo studies revealed that these novel integrin-targeting devices efficiently inhibit tumor growth. Thus, the combination of β-diketone derivatives of RGD peptidomimetics that target cell surface integrins $\alpha v\beta 3$ and $\alpha v\beta 5$ with monoclonal aldolase antibodies through formation of a covalent bond of defined stoichiometry holds promise as a new approach to cancer therapy.

Introduction

In recent years, the use of monoclonal antibodies (mAbs) for the treatment of various diseases has grown rapidly. This is evident from the availability of a dozen of therapeutic mAbs recently approved by the U.S. Food and Drug Administration, as well as a considerable number of therapeutic mAbs that are in clinical trials.[1] Distinctive features of the antibody molecule that are important for therapeutic applications include antigen binding with high specificity and affinity, antibody-dependent cellular cytotoxicity (ADCC),[2] and long serum half-life.[3] We reasoned that these features of mAbs can be combined in a complementary fashion with the diversity of low molecular weight compounds, which could potentially surpass mAbs in terms of specificity, affinity, and avidity of antigen binding.[4] Specifically, we focused our attention to a group of mAb conjugates that were derived from the combination of catalytic aldolase mAb 38C2 and integrin $\alpha v\beta 3$ and $\alpha v\beta 5$-targeting synthetic RGD peptidomimetics.

Aldolase antibody 38C2 and related catalytic mAbs that were generated by reactive immunization[5] catalyze aldol and retro-aldol reactions of diverse substrates. Hapten **1** (Figure 1A) was used as reactive immunogen in the generation of aldolase antibody 38C2. Its electrophilic β-diketone functionality served to induce the generation of mAbs, which display in their hapten binding site a nucleophilic amine group that can covalently bind the β-diketone to form an enaminone (Figure 1A). The nucleophilic amine group in the hapten binding site of mAb 38C2 and other aldolase antibodies was identified as the ϵ-amino group of a lysine residue activated by burial in a hydrophobic pocket.[6] This reactive lysine is essential for the catalytic activity of these aldolase antibodies. Alongside their use in natural product syntheses,[7] aldolase antibodies have been employed for selective prodrug activation in vitro and in vivo.[8] However, their unique feature of covalently interacting with a β-diketone functionality merits a range of novel applications in the growing field of

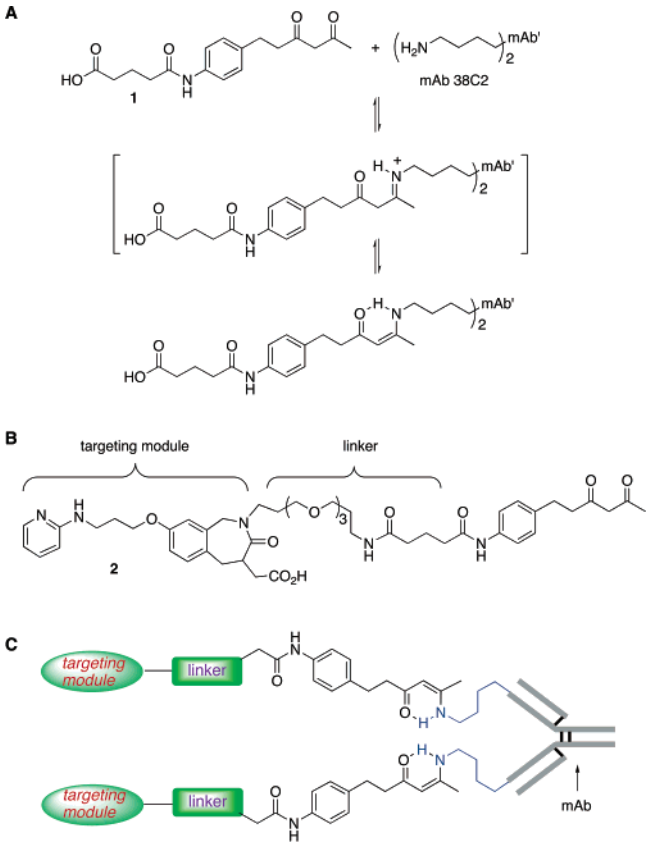

Figure 1. (A) Enamine formation of diketone compound **1** with mAb 38C2 to form the enaminone derivative via the corresponding iminium salt. (B) Structure of a representative targeting molecule, **2**. (C) Schematic drawing of the device assembled from a targeting molecule and mAb 38C2.

* To whom correspondence should be addressed. Phone, (858) 784-8512; fax, (858) 784-8732; e-mail, subhash@scripps.edu.

† Present address: Experimental Transplantation and Immunology Branch, Center for Cancer Research, National Cancer Institute, National Institutes of Health, 9000 Rockville Pike, Bethesda, MD 20892-1907.

10.1021/jm049666k CCC: $27.50
Published on Web 10/06/2004

interface molecules that consist of a protein component covalently linked to a synthetic component.[9] Exploiting this, we reasoned that the attachment of the β-diketone functionality to an RGD peptidomimetic would allow us to program mAb 38C2 with the integrin targeting properties. The resulting conjugate as shown in Figure 1B differs from conventional antibody conjugates in that (i) the synthetic component and not the antibody binds the target and (ii) the conjugation is highly defined by selectively engaging only the two reactive lysine residues of the antibody molecule. As a consequence, our design allows for the chemical programming of mAb 38C2 with the targeting modules in a stoichiometrically defined way, in which only the reactive lysine residues in the two binding sites of the mAb but not any other residues are modified. This feature of our approach makes the resultant antibody conjugate superior to conventional antibody conjugates, in which the mAb is randomly derivatized through surface lysine residues, cysteine residues, or aldehydes generated from oxidation of carbohydrates in the Fc region.[10]

We set out to test our concept using targeting modules that selectively bind integrins $\alpha v\beta 3$ and $\alpha v\beta 5$. As a proof of concept, we developed compound **2**, a β-diketone derivative of an RGD peptidomimetic that selectively binds to $\alpha v\beta 3$ and $\alpha v\beta 5$ integrins. In a preliminary report,[11] we showed that **2** covalently bound to monoclonal aldolase antibody 38C2 and in doing so programmed the antibody to target tumor and endothelial cells that express integrins $\alpha v\beta 3$ and $\alpha v\beta 5$. In vivo, the complex of **2** and mAb 38C2 was shown to assemble spontaneously to increase the half-life of **2** in circulation by more than 2 orders of magnitude and effectively reduce tumor growth in mouse models. Here, we report design, synthesis, and assembly of a series of novel integrin-targeting devices using β-diketone derivatives of RGD peptidomimetics including **2** and their ability to program mAb 38C2 for targeting human melanoma and metastatic breast cancer cells.

Results and Discussion

Integrins $\alpha v\beta 3$ and $\alpha v\beta 5$ are expressed on the cell surface of tumor infiltrating endothelial cells as well as certain tumor cells and have become investigational molecular targets for cancer therapy in a growing number of clinical trials.[12] Hence, a number of RGD peptides, peptidomimetics,[13] and mAbs[14] have been developed that efficiently target integrins $\alpha v\beta 3$ or $\alpha v\beta 5$. RGD peptide antagonists have also been used efficiently to deliver cytotoxic drugs,[15] transport polyamines for delivery of gene therapy agents,[16] and transport imaging agents for tumor therapy.[17] These αv integrins as well as the related integrin $\alpha IIb\beta 3$ bind to a diverse set of extracellular matrix proteins largely through interaction with an RGD tripeptide binding site. Initial discovery of the integrins $\alpha v\beta 3$- and $\alpha v\beta 5$-targeting RGD peptides as well as synthetic RGD peptidomimetics[18] was based on already known skeletons of the antgagonists of integrin $\alpha IIb\beta 3$. Subsequently, a number of synthetic RGD peptidomimetics, including Smith Kline Beecham (SKB) compounds **3**−**5**[19] and Merck compound **6**[20] (Figure 2), were developed, which bind very tightly to the αv integrins and virtually do not bind to $\alpha IIb\beta 3$. Thus, these compounds promised to be suitable integrin binding moieties for the design of a targeting module that, by conjugation to mAb 38C2, would program the antibody for selective targeting of cells expressing the αv integrins.

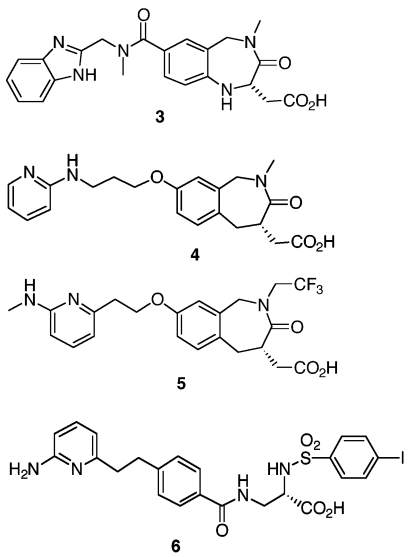

Figure 2. Structure of RGD peptidomimetics developed by Smith-Kline Beecham (**3**−**5**) and Merck (**6**).

Synthesis of RGD Peptidomimetics Designed for Antibody Docking. We designed and synthesized targeting modules based on the integrin binding cores of RGD peptidomimetics **3**−**6**. Initially, we focused on analogues of the SKB compounds **3**−**5**. To incorporate a β-diketone functionality that would allow mAb docking but would not interfere with integrin binding, a linker arm was designed. The location of the linker arm was determined on the basis of a study of a large number of published analogues of SKB compounds **3**−**5** and their structure−activity relationships. Both polymethylene and PEG linkers were studied. Figure 3 shows the structure of the synthesized targeting modules **2** and **7**−**12** that were based on the SKB compounds and contained a β-diketone or biotin functionality. Biotin derivatives **11** and **12** were synthesized (i) for controls and (ii) to compare their noncovalent docking to an anti-biotin mAb with the covalent docking of the corresponding β-diketone derivatives to mAb 38C2.

Compounds **2** and **7**−**12** were synthesized via their intermediates **13**−**16** (Schemes 1 and 2). The latter compounds were prepared by modifying the synthesis of the parent SKB compounds **3**−**5** to accommodate the linker groups. Thus, as shown in Scheme 1, the known bromide **31** was reacted with mono-Boc-protected ethylenediamine (**32**). The resultant product **33** was amidated using aspartic acid derivative **34**, giving **35**. The latter was subjected to hydrogenolysis, and the free amine was then cyclized at high temperature under dilute conditions to provide **36**. Both Boc and *tert*-butyl protecting groups in **36** were cleaved using TFA, and the product was reacted with *N*-Boc-protected 6-aminohexanoic acid NHS ester linker (**37**) to afford **38**. Acid **38** was amidated with amine **39**, and the product **13a** was hydrolyzed using aqueous NaOH to afford the first precursor, **13**. In a similar manner, compound **14** was prepared starting from **31** via **41** that was prepared by reaction of the former with mono-Boc-protected 4,7,10-trioxatridecane-1,13-diamine, **40**. Compound **41** was

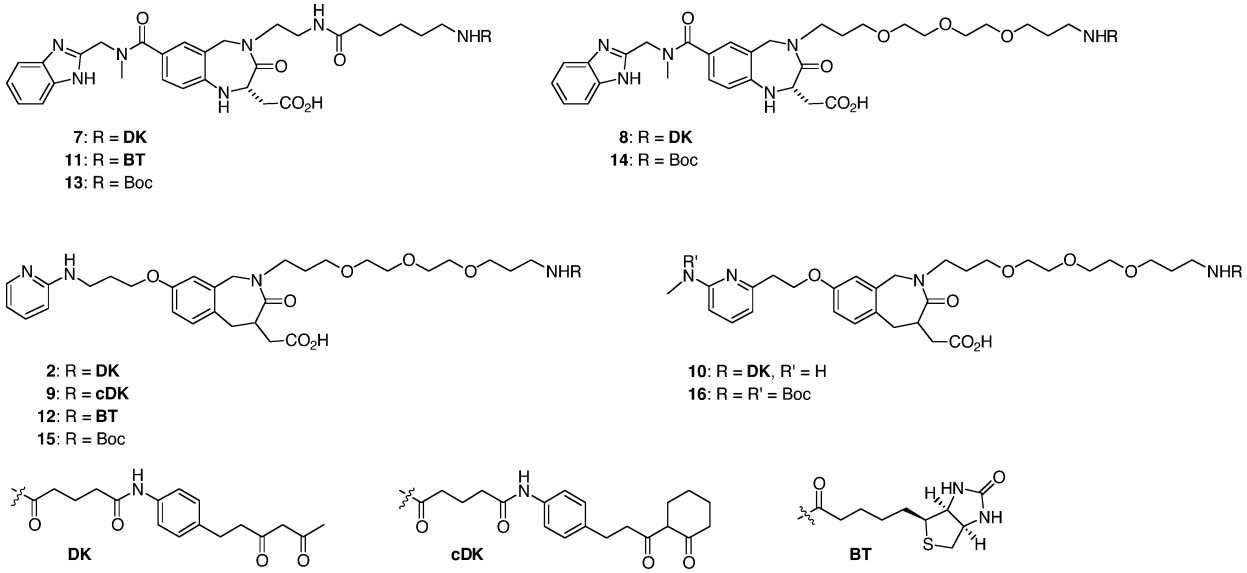

Figure 3. Synthesized analogues of SKB molecules **2** and **7**−**12**, which are equipped with a β-diketone or biotin functionality and designed to allow integrin binding and mAb docking at the same time, and their precursors (**13**−**16**).

Scheme 1. Synthesis of Targeting Modules Equipped with β-Diketone or Biotin Functionalities, **7**, **8**, and **11**[a]

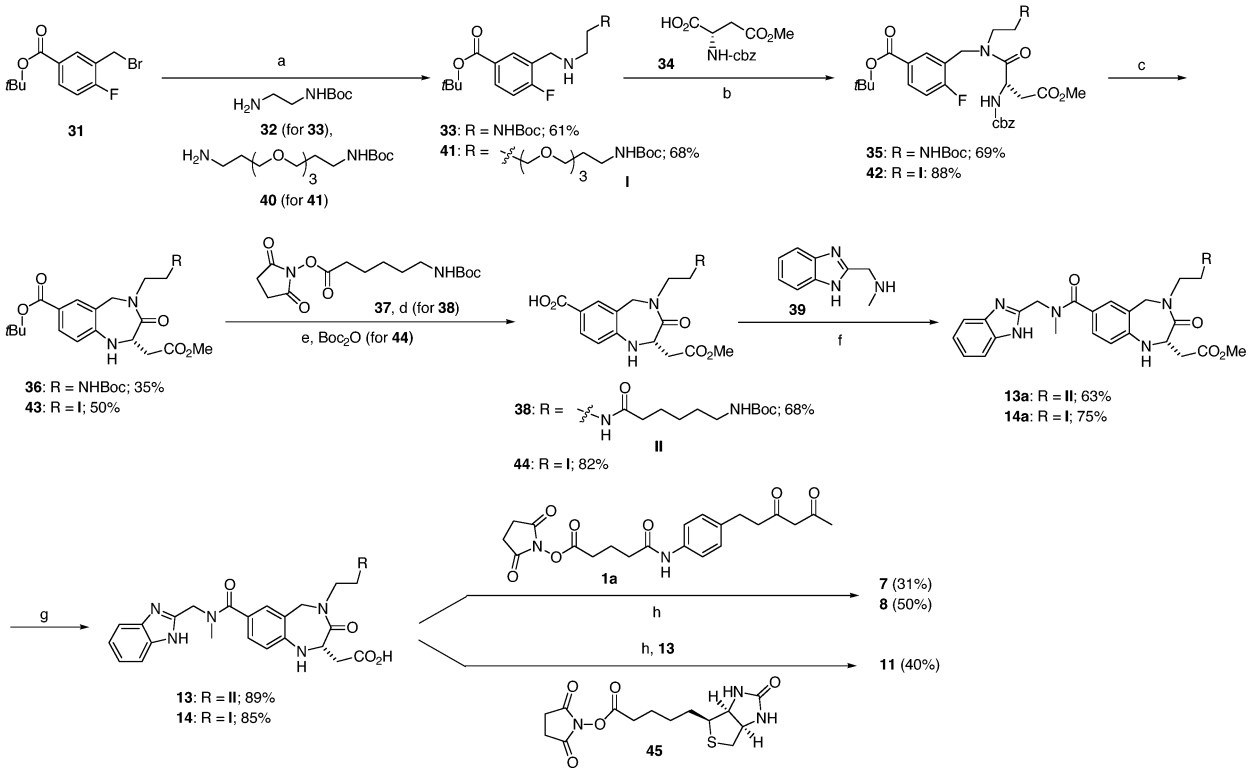

[a] Key: (a) DMF, room temp; (b) EDC, HOBT, DMF; (c) (i) H_2, Pd−C (10%, w/w), EtOH, (ii) 0.01 M in DMSO, Δ; (d) (i) TFA, anisole, CH_2Cl_2, (ii) i-Pr_2NEt, DMF; (e) (i) TFA, anisole, CH_2Cl_2, (ii) $(Boc)_2O$, $NaHCO_3$, THF; (f) EDC, HOBT, DMF; (g) 2 M NaOH, MeOH−THF (1:1); (h) (i) TFA, anisole, CH_2Cl_2, (ii) Et_3N, CH_3CN, room temp.

amidated with **34**, and the amide **42** was cyclized after hydrogenolysis to afford **43**. The product obtained from the acid (TFA) treatment of **43** was reacted with $(Boc)_2O$ to reprotect the free amine function, and the resultant acid **44** was amidated with **39** to give **14a**, which was then hydrolyzed under basic conditions to afford **14**. Compounds **13** and **14** were treated with TFA, and the products were then reacted with the activated diketone (**1a**) or biotin (**45**) compounds to afford **7**, **8**, and **11**.

Syntheses of the SKB compounds **4** and **5** based molecules are shown in Scheme 2. The syntheses started from the known bromide **46a**. The methoxy group was deprotected and then reprotected as TBDPS ether to afford **46b**. The latter product was reacted with mono-Boc-protected 4,7,10-trioxatridecane-1,13-diamine, **40**, followed by cbz-chloride to afford **47**. Compound **47** underwent Heck arylation with dimethyl itaconate, and the resultant product **48** was hydrogenated using Pd−C

Scheme 2. Synthesis of Targeting Modules Equipped with β-Diketone or Biotin Functionalities, **2**, **9**−**10**, and **12**[a]

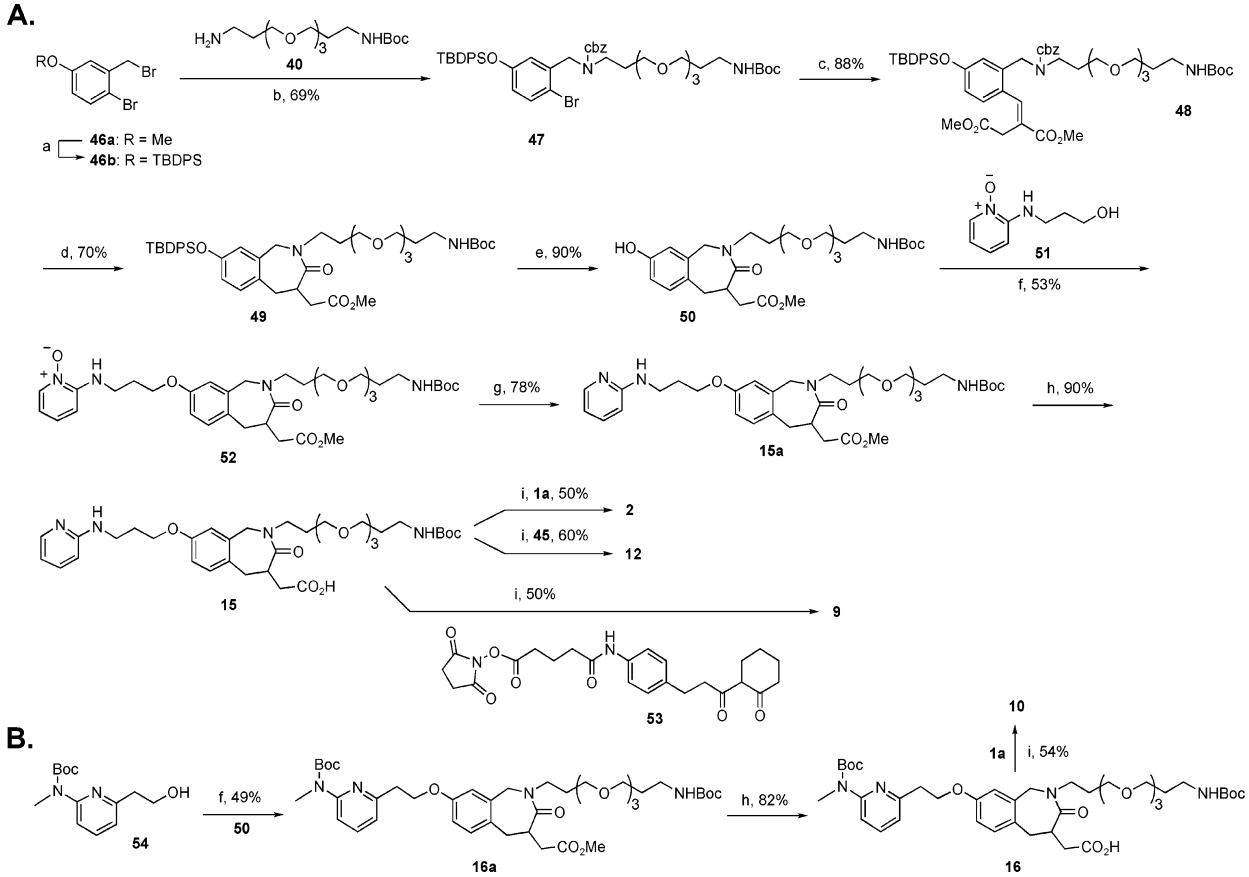

[a] Key: (a) (i) BBr_3, CH_2Cl_2, (ii) TBDPSCl, imidazole, DMF; (b) (i) DMF, room temp, (ii) cbzCl, saturated aqueous $NaHCO_3$, ether, 0 °C; (c) dimethyl itaconate, $Pd(OAc)_2$, (*o*-tol)$_3$P, *i*Pr_2EtN, CH_3CH_2CN, 90 °C; (d) (i) H_2, Pd−C (10% w/w), EtOH−AcOH (1:1), (ii) *i*Pr_2NEt, xylene, 120 °C, 3 h; (e) TBAF, THF, room temp, 1 h; (f) DEAD, PPh_3, THF−benzene (3:1), 16 h; (g) Pd−C (10% w/w), cyclohexene−*i*PrOH (1:1); (h) aqueous (2 N) NaOH, MeOH−THF (1:1), (i) (i) TFA, anisole, CH_2Cl_2, (ii) Et_3N, CH_3CN, room temp.

catalyst in 1:1 solution of EtOH−AcOH. The crude product was cyclized without purification to afford **49**. The TBDPS ether in the cyclized compound **49** was cleaved, and the free phenol **50** then underwent Mitsunobu reaction with alcohol **51** to provide **52**. The *N*-oxide function was reduced, and the ester function in product **15a** was hydrolyzed under basic conditions to afford **15**, the precursor of compounds **2**, **9**, and **12**. The latter compounds were obtained as before by Boc deprotection in **15** using TFA, followed by treatment with the activated esters **1a**, **53**, and **45**, respectively. For the synthesis of compound **16**, alcohol **54** underwent Mitsunobu reaction with phenol **50** to afford **16a**. Basic hydrolysis of **16a** afforded **16**, which was deprotected and reacted with **1a** to afford **10**.

On the basis of the Merck compound **6**, we designed and synthesized the β-diketone compounds **17**−**23** (Figure 4). Broadly, three types of derivatives were prepared. These differed from each other in the positioning of the linkers, which were attached at three locations. In compounds **17**−**19**, the linker was introduced in the benzoic acid core. In compounds **20** and **21** the linker was attached to the aspartic acid mimic, and in compounds **22** and **23** the linker was attached to the guanidine-mimic nitrogen.

Compounds **24**−**30**, the precursors of diketones **17**−**23**, were synthesized by modifying the synthesis of the Merck compound **6** to accommodate the linker groups and then converted to **17**−**23** as described in Schemes 3 and 4. Scheme 3 shows the synthesis of compounds **17**−**19** via **24**−**26** starting from iodides **58a**,**b** that were prepared by Mitsunobu reaction of phenol **55** with alcohols **56** and **57**, respectively. Sonogashira palladium-catalyzed cross coupling of **58a**,**b** with TMS-acetylene followed by removal of the silyl protecting group afforded alkynes **59a**,**b**. The latter compounds underwent second Sonogashira coupling with bromide **60b**, and the resultant alkynes **61a**,**b** were hydrogenated to afford **62a**,**b**. Compounds **62a**,**b** were hydrolyzed using aqueous base, and the products **63a**,**b** were amidated with amine **64a** to give **24** and **25**, respectively. Compound **26** was prepared from **62b** in four steps. First, the Boc protecting group was cleaved using TFA, then the product was reacted with the *N*-Boc 6-aminohexanoic acid NHS ester (**37**) to afford **65**. The methyl ester of **65** was hydrolyzed, and finally the resultant acid was amidated with **64a**. Conversion of the intermediates **24**−**26** to **17**−**19** was achieved in two steps. Thus, the Boc and *tert*-butyl groups in **24**−**26** were deprotected using a mixture of TFA and anisole in dichloromethane, and the resultant amino acids were then reacted with the NHS ester of the β-diketone compound, **1a**.

Syntheses of precursors **27**−**30** of the remaining targeting molecules **20**−**23** are shown in Scheme 4. Compound **68a** has been previously synthesized starting from bromides **60a** and alkyne **66** via alkyne **67a**.[20] In an analogous manner compounds **68b** and **68c** were also prepared from **60b**,**c** and **66** via alkynes **67b**,**c**. Acid **68b**

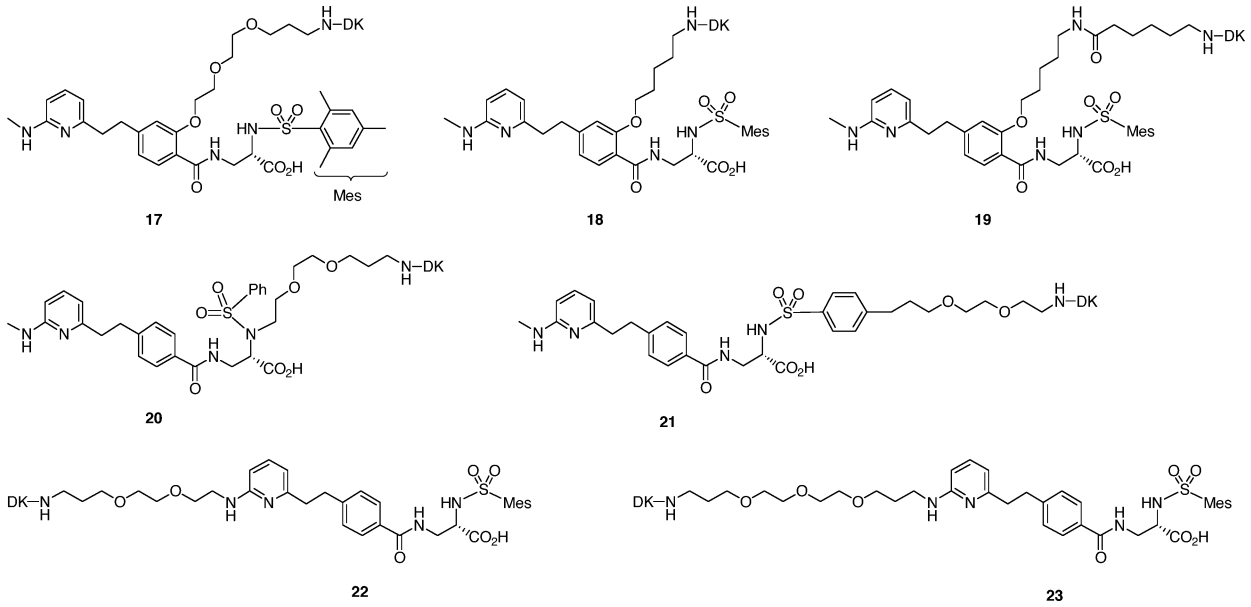

Figure 4. Structure of derivatives of Merck compound **6** equipped with a β-diketone functionality (**17**−**23**, DK = diketone; see Figure 3).

Scheme 3. Synthesis of Targeting Modules Equipped with a β-Diketone Functionality, **17**−**19**[a]

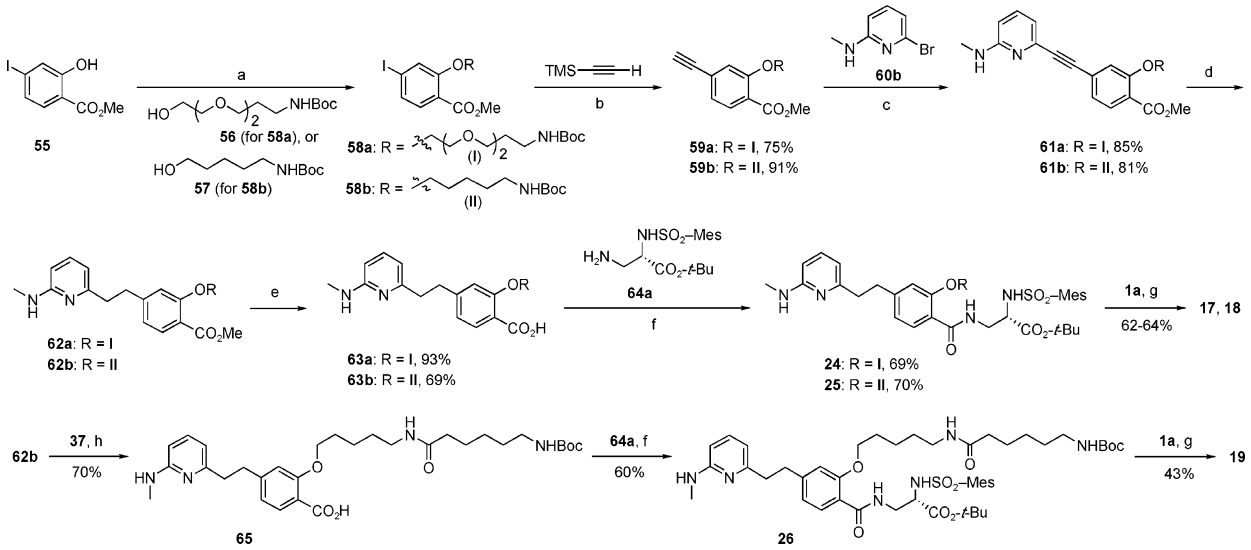

[a] Key: (a) PPh_3, DIAD, CH_2Cl_2, 0 °C to room temp, 16 h; (b) (i) $Pd(PPh_3)_2Cl_2$, CuI, Et_3N, EtCN, 90 °C, 16 h, (ii) K_2CO_3, MeOH, room temp, 2 h; (c) $Pd(PPh_3)_2Cl_2$, CuI, Et_3N, EtCN, 90 °C, 16 h; (d) H_2, 10% (w/w) Pd−C, EtOH, 16 h; (e) aqueous NaOH, MeOH−THF, 16 h, then acetic acid; (f) EDC, HOBT, NMM, DMF, room temp, 16 h; (g) (i) TFA, anisole, CH_2Cl_2, 0 °C, 16 h, then **1a**, Et_3N, CH_3CN, room temp, 2−5 h; (h) (i) TFA, anisole, CH_2Cl_2, room temp, 2 h, then **37**, iPr$_2$NEt, CH_3CN, room temp, 2 h (ii) step e.

was reacted with amine **64b**, and the resultant product **69** was N-alkylated using alcohol **56** under Mitsunobu conditions to give **27**. Similarly, **68c** was amidated using **64a** to afford **30** (Scheme 4A). For the synthesis of compound **29**, amine **68a** was alkylated by imine formation with aldehyde **70** followed by reduction with $NaCNBH_3$ to afford **71**, which was then amidated using amine **64a** (Scheme 4B). The remaining precursor, **28**, was prepared by amide formation between amine **64c** and acid **68b** (Scheme 4C). Conversion of the intermediates **27**−**30** to **20**−**23** was achieved in two steps by deprotection of Boc and *tert*-butyl groups in **27**−**30** using a mixture of TFA and anisole followed by reaction of the resultant amino acids with **1a** (Scheme 4), as described before for the synthesis of compounds **17**−**19** (Scheme 3).

Antibody Docking. Aldolase antibody 38C2 reacts covalently, yet reversibly, through its two reactive lysine residues with β-diketone compounds to produce the corresponding enaminone derivatives. Both enaminone formation and the reversibility of the reaction between mAb 38C2 and β-diketone compounds were confirmed by UV and surface plasmon resonance, respectively.[21] To determine whether our synthesized targeting modules with β-diketone functionality, compounds **2**, **7**−**10**, and **17**−**23,** would also covalently dock to the reactive lysine residues of mAb 38C2, a selection of compounds was incubated with 0.5 equiv of mAb 38C2 for 30 min at room temperature, and the catalytic activity of the mixture was analyzed using methodol as aldol sensor.[22] Using a fluorescence reader, we found that our synthesized targeting modules with β-diketone functionality

Scheme 4. Synthesis of Targeting Modules Equipped with a β-Diketone Functionality, **20**−**23**[a]

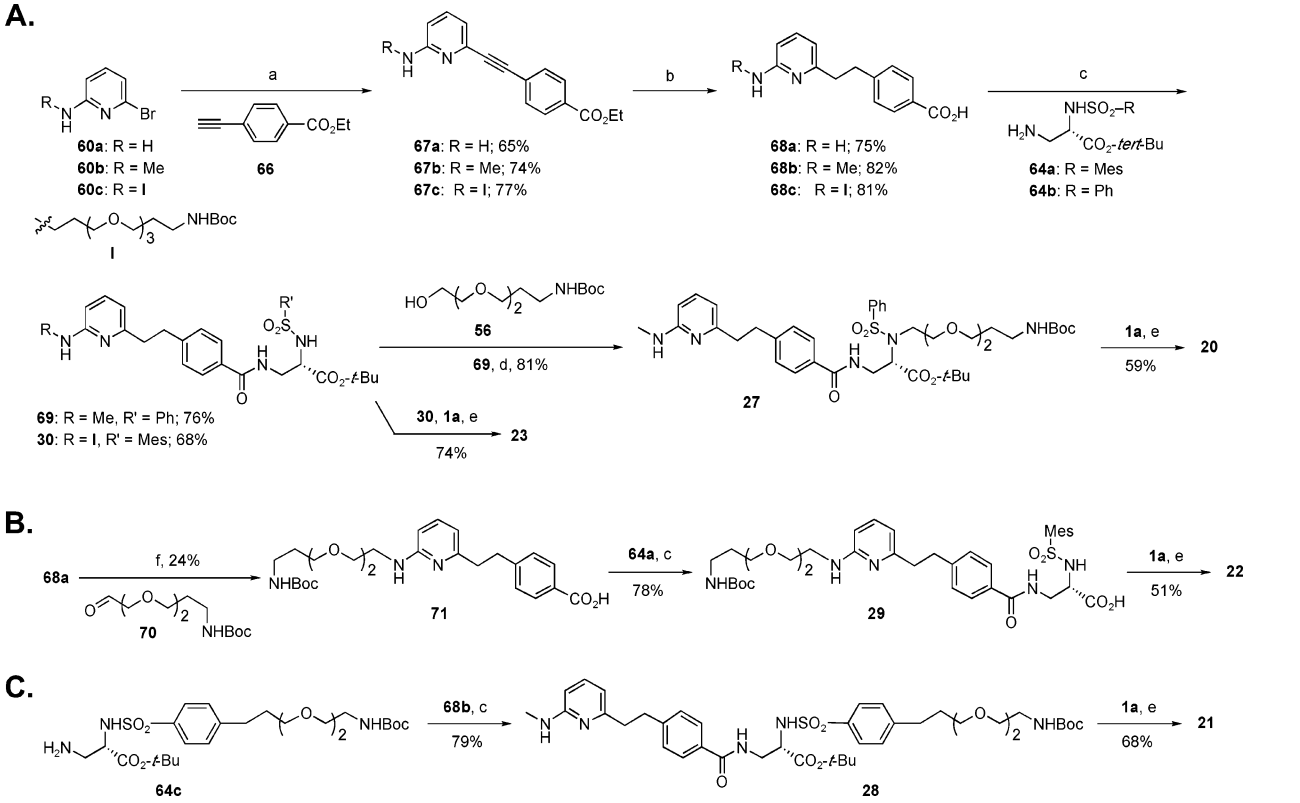

[a] Key: (a) $Pd(PPh_3)_2Cl_2$, CuI, Et_3N, EtCN, 90 °C, 16 h; (b) (i) H_2, 10% (w/w) Pd−C, EtOH, 16 h, (ii) aqueous NaOH, MeOH−THF, 16 h, then acetic acid; (c) EDC, HOBT, NMM, DMF, room temp, 16 h; (d) PPh_3, DIAD, CH_2Cl_2, 0 °C to room temp, 16 h; (e) (i) TFA, anisole, CH_2Cl_2, 0 °C, 16 h, then **1a**, Et_3N, CH_3CN, room temp, 2−5 h; (f) molecular sieves (3Å), CH_2Cl_2−DMF (1:1), room temp, 4 h, then $NaCNBH_3$, 0 °C to room temp, 16 h.

completely inhibited the aldolase activity of mAb 38C2 (data not shown). Targeting modules with biotin functionality, by contrast, did not affect the catalytic activity of mAb 38C2. The observation that the catalytic activity of 0.5 equiv of mAb 38C2 could be completely shut down with only 1 equiv of a targeting module with β-diketone functionality reveals a simultaneous docking to both reactive lysine residues of the antibody molecule.

Integrin Targeting. Next we tested whether the synthesized targeting modules can direct the binding of docked mAbs to cells expressing integrin $\alpha v\beta 3$ and/or integrin $\alpha v\beta 5$ on their surface. The binding of conjugates derived from varying concentration (1×, 2×, and 4× molar ratios) of β-diketone **7** and mAb 38C2 was evaluated by flow cytometry using integrin $\alpha v\beta 3$ expressing human melanoma cell line M21. As shown in Figure 5, compound **7** effectively mediated the binding of mAb 38C2 to the cell surface in a dose-dependent manner that likely reflects the occupation of the two active sites of the antibody molecule. By contrast, mAb 38C2 in the absence of compound **7** did not bind the cell surface. Similarly, conjugates obtained by incubating β-diketone compounds **7** or **2** with mAb 38C2 efficiently bound to a human Kaposi's sarcoma cell line, which expresses both integrins $\alpha v\beta 3$ and $\alpha v\beta 5$.[11] Again, binding of mAb 38C2 alone or compound **7** or **2** alone was not detected.

To further analyze the selectivity of conjugate formation, we analyzed the programming of three different mAbs by three RGD peptidomimetics equipped with different docking functionalities (Figure 6). Compounds

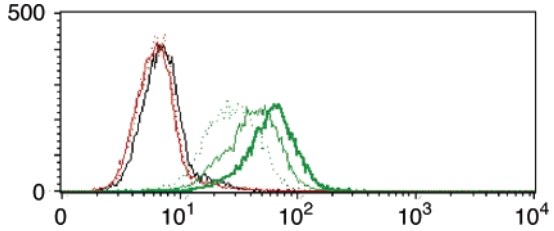

Figure 5. Flow cytometry histogram showing the binding of mAb 38C2 to integrin $\alpha v\beta 3$ expressing human melanoma cell line M21 in the absence and presence of compound **7**. Antibody 38C2 was used at 25 μg/mL after preincubation with compound **7** in half equimolar (dotted green line), equimolar (thin green line), and twice equimolar (bold green line) concentration. The negative controls were 25 μg/mL mAb 38C2 alone (thin red line), twice equimolar compound **7** alone (dotted red line), and secondary antibody alone (thin black line). In all experiments, FITC-conjugated goat antimouse secondary antibodies were used for detection. The *y* axis gives the number of events in linear scale, and the *x* axis is the fluorescence intensity in logarithmic scale.

2 and **9** display the β-diketone functionality as acetone and cyclohexyl β-diketone analogue, respectively, whereas compound **12** contains a biotin functionality. As shown in Figure 6A, mAb 38C2 was programmed by compound **2** and, less efficiently, by compound **9** for cell surface targeting, reflecting a higher K_M of mAb 38C2 for cyclohexyl β-diketones.[23] As expected, biotin compound **12** was incapable of programming mAb 38C2. Neither compound was capable of programming control mAb 26G10, which has the same isotype (mouse IgG2a) as mAb 38C2 (Figure 6B). By contrast, anti-biotin mAb

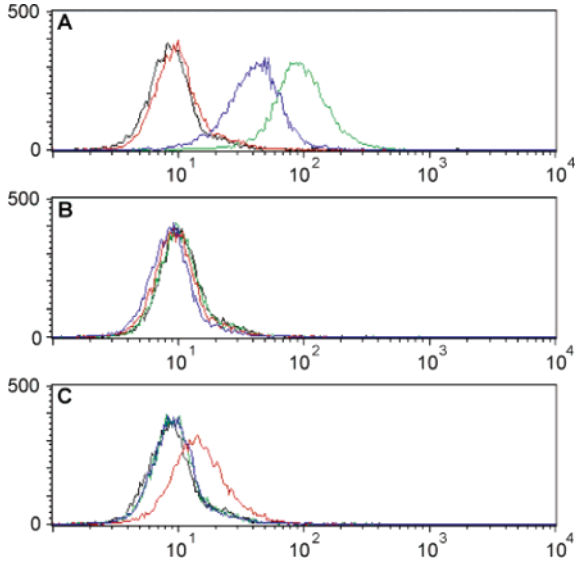

Figure 6. Flow cytometry histograms showing the binding of (A) mAb 38C2, (B) control mAb 26G10, and (C) anti-biotin mAb BN34 to metastatic human breast cancer cell line MDA-MB-435 in the absence (black line) or presence of a twice equimolar concentration of compounds **2** (green line), **9** (blue line), and **12** (red line). In all experiments, FITC-conjugated goat antimouse secondary antibodies were used for detection. The *y* axis gives the number of events in linear scale, and the *x* axis is the fluorescence intensity in logarithmic scale.

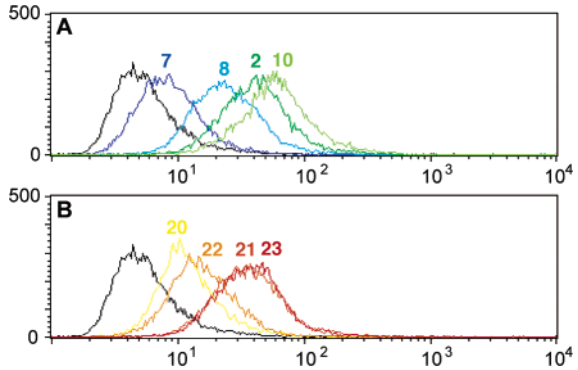

Figure 7. Flow cytometry histograms showing the binding of mAb 38C2 to integrin $\alpha_v\beta_3$ and $\alpha_v\beta_5$ expressing MDA-MB-435 human breast cancer cells in the absence (black line) and presence (colored lines) of a twice equimolar concentration of (A) SKB-based compounds **2**, **7**−**8** and **10** and (B) Merck-based compounds **20**−**23**. In all experiments, FITC-conjugated goat antimouse secondary antibodies were used for detection. The *y* axis gives the number of events in linear scale, and the *x* axis is the fluorescence intensity in logarithmic scale.

BN34 (Sigma-Aldrich) was programmed by biotin compound **12** but not by *β*-diketone compounds **2** and **9** (Figure 6C). Although the covalent conjugations involving mAb 38C2 compared favorably to the noncovalent conjugate formed by mAb BN34 and compound **12** (Figure 6A vs Figure 6C), the latter proves the general applicability of our targeting strategy.

SKB compounds **3** and **4**, the parent molecules of *β*-diketone compounds **7** and **2**, respectively, were shown to bind to integrins αv*β*3 and αv*β*5 with comparable affinity.[19] Yet, as shown in Figure 7A, we found that compound **7** mediated binding of mAb 38C2 to MDA-MB-435 human breast cancer cells less efficiently than compound **2**. This finding could be explained by the

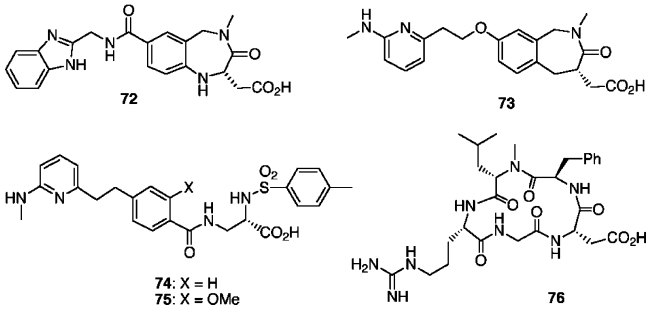

Figure 8. Structure of SKB-type molecules (**72** and **73**), Merck-type molecules (**74** and **75**), and RGD peptide (**76**) used in the docking studies.

different linker compositions, polymethylene versus PEG, that separate the integrin binding core from the *β*-diketone functionality in compounds **7** and **2,** respectively (Figure 3). In fact, replacing the polymethylene linker of compound **7** with a PEG linker yielded compound **8**, which revealed improved mAb 38C2 programming (Figure 7A). On the basis of the apparent superiority of the PEG linker, our second generation of *β*-diketone compounds, based on SKB compound **5** and Merck compound **6**, was equipped with PEG linkers. Compound **10**, which was based on SKB compound **5**, was found to be the most efficient mediator of cell surface binding (Figure 7A).

A comparison of *β*-diketone compounds based on Merck compound **6** is shown in Figure 7B. Compounds **21** and **23**, which have the linker plus *β*-diketone functionality attached to opposite sites of the integrin binding core (Figure 4), were able to mediate the binding of mAb 38C2 to MDA-MB-435 human breast cancer cells with an efficiency comparable to that of compound **2**. Interestingly, compound **22**, which differs from compound **23** in that it possesses a shorter PEG linker, was notably less efficient, suggesting that linker length is a critical parameter in allowing the compound to simultaneously bind the antibody and the cell surface receptor. By contrast, compounds **17**−**19**, in which the linker is attached through the core phenyl ring (Figure 4), were inactive (data not shown) and compound **20**, in which the linker is attached to the nitrogen atom rather than to the phenyl ring of the aspartic acid mimetic (Figure 4), was less efficient than compound **21** (Figure 7B). These results provide clear instructions on how Merck compound **6** can be derivatized without affecting its integrin binding capability.

Molecular Docking Study. To probe our results of the placement of linker plus *β*-diketone functionality to the above-described RGD peptidomimetics in different positions, we carried out molecular docking studies using structures **72**−**76** (Figure 8). Here, compounds **72** and **73** represented the SKB-type molecules **2** and **7**−**12**, and compounds **74** and **75** represented the Merck-type molecules **17**−**23**. In earlier studies, several groups have performed molecular docking calculations using various RGD peptides and peptidomimetics, including **3**, **4**, and **6**.[24,25] These molecular docking studies were conducted using AutoDock 3.0.5 program[26] on the basis of the published crystal structure of the extracellular portion of the integrin αv*β*3 heterodimer alone[27] or in complex with a cyclic RGD pentapeptide, **76**,[28] in addition to photoaffinity cross-linking studies.[29] We used the crystal

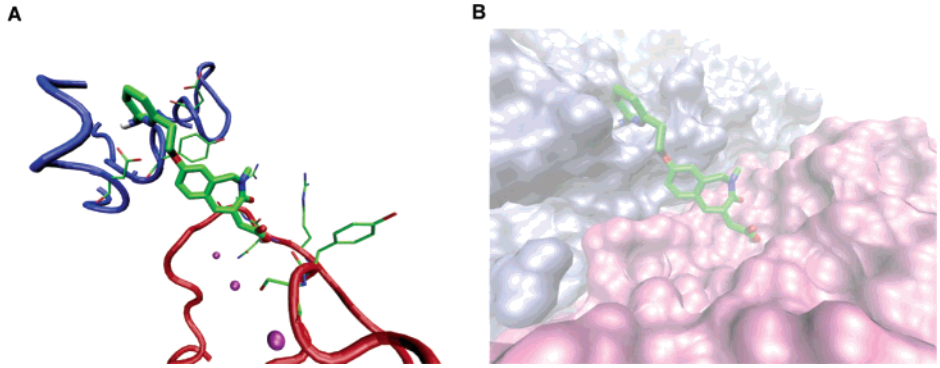

Figure 9. Projected binding mode of compound **73**, an SKB compound, in the binding site of integrin αvβ3 based on docking studies using AutoDock tool.

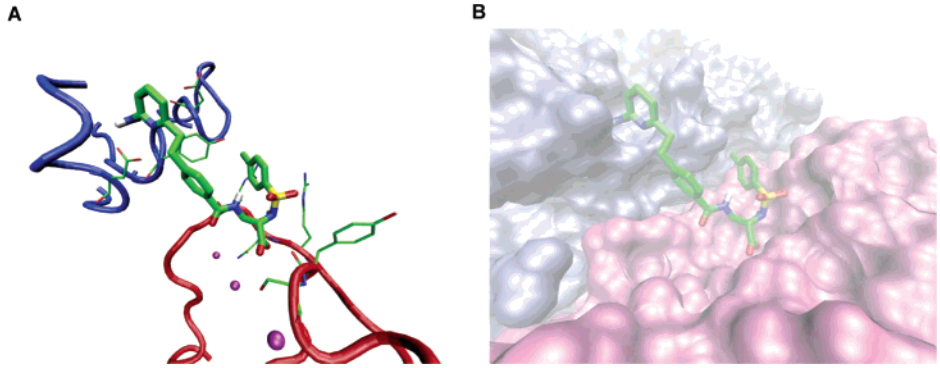

Figure 10. Projected binding mode of compound **74**, an analogue of Merck compounds, in the binding site of integrin αvβ3 based on docking studies using AutoDock tool.

structure data of the integrin−ligand complex for our molecular docking studies, which have been shown to successfully reproduce the experimentally observed binding mode. The methods of calculation were similar to those previously described by Kessler et al.[25b] except that the calculated binding mode of the antagonists was not minimized further (see Supporting Information for the details).

Initially, we performed the docking calculations with structure **76** to reproduce the observed binding mode of the cyclic RGD peptide in the crystal structure of the integrin−ligand complex.[28] We also calculated the molecular docking of compound **72** and compared the results with the published data by Kessler et al.[25b] Molecular docking of both **72** and **76** was in close agreement with the reported data (see Supporting Information). Next, we calculated the molecular docking of compounds **73** and **74**, the results of which are shown in Figures 9 and 10, respectively. Both the structures **73** and **74** represented a binding mode identical to that of cyclic RGD ligand **76** and SKB molecule **72** in each case. This binding mode for **73** was among the first three preferred solutions for **73** with the third lowest free energy of binding (E = −8.54 kcal/mol) and involves carboxylate oxygen complexation with the Ca^{2+} ion at the MIDAS region in the β chain, whereas the aminopyridine side chain inserts into a narrow groove at the top of the propeller domain of the α chain. The benzodiazepine ring lies at the interface between the α and β subunits, whereas the *N*-methyl group points outside the receptor surface, which makes the methyl function a suitable location for incorporating the linker. In fact, the methyl function in **73** points away from the receptor surface in all three preferred binding modes. For the Merck-type molecule **74**, the binding mode depicted in Figure 10 has the lowest free energy of binding (E = −8.54 kcal/mol) and is representative of the most populated cluster among the first four preferred clusters. In this mode, the guanidine mimetic group interacts with the regions of Asp150 and Asp218 of the α chain; one of the oxygen of the aspartic acid mimetic group of **74** makes contact with the Ca^{2+} ion, and the other oxygen interacts with the backbone of the Asn 215 of the β chain. In addition, one of the sulfonamide oxygen forms a hydrogen bond with the guanidine group of Arg214 in the β chain and the internal phenyl ring of **74** possesses a $\pi-\pi$ stacking interaction with Tyr178 of the α chain. Moreover, both the guanidine "N" and the 4-position on the benzenesulfonamide were found to be suitable locations for linker placement in the Merck-type molecules. Failure of the benzene ring based linker derivatives of these molecules as evident from our binding assays was further supported by molecular docking calculations with compound **75**.

In Vivo Studies. In a study we published elsewhere,[11] the complex formed by mAb 38C2 and β-diketone compound **2** was shown to spontaneously assemble not only in vitro but also in vivo after injecting mAb 38C2 intravenously and compound **2** intraperitoneally into mice. In doing so, mAb 38C2 extended the circulatory half-life of compound **2** by more than 2 orders of magnitude. We also found that the complex, in contrast to mAb 38C2 or compound **2** alone, effectively reduced tumor growth in mouse xenografts modeling human Kaposi's sarcoma and colon cancer. Interestingly, whereas the human Kaposi's sarcoma cells (SLK)

expressed integrins αvβ3 and αvβ5, the xenografted human colon cancer cells (SW1222) did not. We suggested that the colon cancer inhibiting activity of the complex is due to an inhibition of mouse endothelial cells that express integrins αvβ3 and/or αvβ5 and infiltrate the human xenograft in a process known as tumor angiogenesis. In support of the suggested antiangiogenic effect, we showed that the complex formed by mAb 38C2 and β-diketone compound **2** binds to mouse and human endothelial cells and inhibits their proliferation in vitro. For cancers in which both tumor and tumor endothelial cells express integrins αvβ3 and/or αvβ5, such as in our Kaposi's sarcoma, the complex is likely to exhibit a dual antitumor and antiangiogenic effect. Similar effects were also noticed by Kok et al. based on a conventional mAb conjugate in which cyclic RGD peptide c(RGDfK) was conjugated to a mAb through surface lysine residues.[30]

In conclusion, by weaving together synthetic chemistry and antibody technology, we developed a conceptually novel class of antibody therapeutics. In essence, a generic antibody molecule was programmed using a diverse set of RGD peptidomimetics for targeting the cell surface protein integrins αvβ3 and αvβ5. Both components of this system, antibodies as well as the RGD peptidomimetics, have been successfully used as therapeutics in general and for cancer therapy in particular. However, a blend of these diverse components promises RGD-based therapeutics with a generic effector element in a defined formulation. In our prototypes described here, the reactive lysine residue in the active site of aldolase antibody 38C2 forms a covalent bond with a β-diketone functionality that was linked to RGD peptidomimetics. These prototypes were found to be efficient in terms of (i) spontaneous complex formation in vitro and in vivo, (ii) cell surface targeting, (iii) circulatory half-life extension, and (iv) tumor growth inhibition.

Experimental Section

All nonaqueous reactions were carried out under an argon atmosphere with commercial grade reagents and freshly distilled solvents. The ^{1}H NMR spectra were recorded on Varian Unity Inova or Bruker instruments. Chemical shifts are reported in ppm relative to tetramethylsilane. Flash column chromatography was performed using EM silica gel 60 (230−400 mesh). Experimental procedures for the synthesis of the precursors and their physical data are briefly described in the Supporting Information.

Compound 7 (General Procedure). Boc deprotection of acid **13** (130 mg, 0.19 mmol) using TFA (0.5 mL) and anisole (0.5 mL) in CH_2Cl_2 (2 mL) afforded the corresponding amine as TFA salt (140 mg), which was used in next step without purification. Compound **1a** (87 mg, 0.2 mmol) was added to a solution of the above-described crude product (140 mg) and Et_3N (0.14 mL) in CH_3CN (2 mL). The mixture was stirred at 0 °C for 4 h and washed with aqueous 10% citric acid, solvents were removed under vaccum, and the residue was purified over silica gel (CH_2Cl_2−MeOH, 19:1 to 4:1). Product was further purified using prep-TLC (CH_2Cl_2−MeOH, 4:1) to afford **7** (50 mg, 31%). ^{1}H NMR (400 MHz, $CD_3OD/CDCl_3$): δ 7.56 (2H, dd, J = 5.8, 3.2 Hz), 7.43 (2H, m), 7.23 (4H, m), 7.10 (2H, d, J = 8.2 Hz), 6.57 (1H, d, J = 7.9 Hz), 5.47 (2H, d, J = 16.4 Hz), 5.13 (1H, t, J = 7.6 Hz), 4.90 (2H, m), 3.88 (1H, d, m), 3.63 (1H, m), 3.43 (1H, m), 3.33−3.20 (4H, m), 3.14 (5H, m), 2.90 (1H, dd, J = 16.4, 8.8 Hz), 2.85 (2H, t, J = 7.6 Hz), 2.60 (1H, dd, J = 16.4, 5.0 Hz), 2.54 (2H, t, J = 7.4 Hz), 2.36 (2H, t, J = 7.3 Hz), 2.24 (2H, t, J = 7.6 Hz), 2.08 (2H, t, J = 7.3 Hz), 1.99 (3H, s), 1.95 (2H, m), 1.52 (2H, m), 1.44 (2H, m), 1.27 (2H, m). MS (ESI), *m/z*: 865 (MH^+), 863 ($M-H)^-$. HRMS (ESI-TOF high acceleration (acc)) calcd for $C_{46}H_{57}N_8O_9$ (MH^+) 865.4243, found 865.4252.

Compound 8. Compound **14** (84 mg, 0.12 mmol) was deprotected using TFA (0.5 mL) and anisole (0.5 mL) in CH_2Cl_2 (2 mL). The crude product was treated with **1a** (54 mg, 0.13 mmol) and Et_3N (0.14 mL) in CH_3CN (2 mL) to afford **8** (55 mg, 50%). R_f = 0.7 (CH_2Cl_2−MeOH, 7:3). ^{1}H NMR (600 MHz, $CD_3OD/CDCl_3$): δ 7.57 (2H, m), 7.45 (2H, m), 7.24 (4H, m), 7.12 (2H, m), 6.60 (1H, d, J = 8.3 Hz), 5.52 (1H, d, J = 15.4 Hz), 5.16 (1H, t, J = 8.8 Hz), 4.87 (2H, m), 3.57−3.52 (7H, m), 3.47 (2H, t, J = 6.1 Hz), 3.44 (3H, m), 3.32 (7H, m), 3.23 (2H, t, J = 7.0 Hz), 3.15 (3H, s), 2.91 (1H, dd, J = 16.6, 8.8 Hz), 2.86 (2H, t, J = 7.9 Hz), 2.82 (1H, s), 2.61 (1H, dd, J = 16.2, 5.2 Hz), 2.58 (2H, t, J = 7.4 Hz), 2.38 (2H, t, J = 7.4 Hz), 2.25 (2H, t, J = 7.0 Hz), 2.01 (3H, s), 1.96 (2H, m), 1.72 (4H, m). MS (ESI), *m/z*: 912.4 (MH^+), 934.4 (MNa^+), 910.4 ($M-H)^-$. HRMS (ESI-TOF high acc) calcd for $C_{48}H_{62}N_7O_{11}$ (MH^+) 912.4502, found 912.4496.

Compound 2.[17] Compound **15** (585 mg, 0.87 mmol) was deprotected using TFA (2.5 mL) and anisole (2.5 mL) in CH_2Cl_2 (10 mL), and the crude product was treated with **1a** (450 mg, 1.1 mmol) and Et_3N (1 mL) in CH_3CN (20 mL) to afford **2** (380 mg, 50%) after purification over silica gel, followed by prep-TLC. R_f = 0.55 (CH_2Cl_2−MeOH, 4:1). HRMS (ESI-TOF high acc) calcd for $C_{47}H_{64}N_5O_{11}$ 874.4597 (MH^+), found 874.4601.

Compound 9. The crude product, obtained after deprotection of compound **15** (100 mg, 0.15 mmol) using TFA (0.5 mL) and anisole (0.5 mL) in CH_2Cl_2 (2 mL), was treated with **53** (75 mg, 0.17 mmol) and Et_3N (0.15 mL) in CH_3CN (2 mL) to afford **9** (68 mg, 50%) after purification over silica gel followed by prep-TLC. ^{1}H NMR (500 MHz, $CDCl_3$): δ 8.92 (1H, s), 7.93 (1H, d, J = 4.4 Hz), 7.48 (3H, m), 7.10 (2H, t, J = 8.5 Hz), 6.97 (2H, m), 6.75 (1H, dd, J = 8.5, 2.6 Hz), 6.64 (1H, d, J = 2.6 Hz), 6.56 (1H, m), 6.46 (1H, d, J = 8.8 Hz), 5.05 (1H, d, J = 16.5 Hz), 4.07 (3H, m), 3.78 (1H, d, J = 16.5 Hz), 3.57 (11H, m), 3.48 (2H, t, J = 4.8 Hz), 3.45 (2H, t, J = 6.3 Hz), 3.61 (5H, m), 2.93 (1H, m), 2.84 (3H, m), 2.67 (2H, t, J = 8.5 Hz), 2.44 (3H, m), 2.37 (2H, t, J = 5.5 Hz), 2.26 (4H, m), 2.09 (2H, m), 2.02 (2H, m), 1.76 (2H, m), 1.72 (2H, m), 1.65 (2H, m).

Compound 10. Compound **16** (72 mg, 0.09 mmol) was deprotected using TFA (0.5 mL) and anisole (0.5 mL) in CH_2Cl_2 (2 mL), and the crude product was treated with **1a** (42 mg, 0.1 mmol) and Et_3N (0.13 mL) in CH_3CN (2 mL). The mixture was washed with 10% citric acid and then purified over silica gel followed by prep-TLC to afford **10** (42 mg, 54%). R_f = 0.6 (CH_2Cl_2−MeOH, 4:1). ^{1}H NMR (600 MHz, $CDCl_3$): δ 8.95 (1H, s), 7.49 (1H, d, J = 8.3 Hz), 7.46 (1H, t, J = 7.9 Hz), 7.08 (2H, d, J = 8.3 Hz), 6.93 (2H, m), 6.71 (1H, m), 6.58 (1H, s), 6.51 (1H, d, J = 7.0 Hz), 6.31 (1H, d, J = 8.3 Hz), 5.06 (1H, d, J = 16.6 Hz), 4.24 (2H, m), 3.73 (1H, d, J = 16.6 Hz), 3.70 (2H, m), 3.60−3.32 (19H, m), 3.08 (2H, t, J = 6.6 Hz), 2.96 (1H, m), 2.87 (3H, s), 2.82 (4H, m), 2.54 (2H, t, J = 7.9 Hz), 2.44 (2H, t, J = 7.2 Hz), 2.28 (2H, t, J = 7.0 Hz), 2.03 (3H, s), 2.01 (2H, m), 1.75 (2H, m), 1.71 (2H, m). MS (ESI), *m/z*: 874 (MH^+), 896 (MNa^+), 872 ($M-H)^-$, 908 ($M+Cl)^-$. HRMS (ESI-TOF high acc) calcd for $C_{47}H_{64}N_5O_{11}$ 874.4597 (MH^+), found 874.4600.

Compound 11. A crude product from the N-deprotection of **13** (30 mg, 0.045 mmol) was treated with **45** (17 mg, 0.05 mmol) and Et_3N (30 μL) in DMF (1 mL). The mixture was purified after treatment with AcOH (0.1 mL) over silica gel using CH_2Cl_2−MeOH followed by PTLC (CH_2Cl_2−MeOH) to afford **11** (14 mg, 40%). ^{1}H NMR (300 MHz, $CDCl_3/CD_3OD$): δ 7.47 (2H, m), 7.25−7.07 (5H, m), 6.44 (1H, d, J = 7.9 Hz), 5.35 (1H, d, J = 16.7 Hz), 5.00 (1H, s), 4.72 (2H, s), 4.37 (1H, m), 4.18 (1H, m), 4.10 (2H, m), 3.4−2.9 (12H, m), 2.8−2.5 (5H, m), 2.07 (2H, m), 1.96 (2H, m), 1.60−1.10 (8H, m).

Compound 12. The crude product, obtained after compound **15** (50 mg, 0.074 mmol) was deprotected using TFA (0.2 mL) and anisole (0.2 mL) in CH_2Cl_2 (0.8 mL), was treated with **45** (30 mg, 0.09 mmol) and Et_3N (80 μL) in DMF (1 mL) to afford **12** (35 mg, 60%) after purification over silica gel using

CH_2Cl_2–MeOH, followed by prep-TLC (CH_2Cl_2–MeOH). ^{1}H NMR (400 MHz, $CDCl_3/CD_3OD$): δ 7.92 (1H, d, J = 4.7 Hz), 7.57 (1H, ddd, J = 8.8, 7.4, 1.8 Hz), 7.01 (1H, d, J = 8.5 Hz), 6.78 (1H, dd, J = 8.2, 2.6 Hz), 6.77 (1H, d, J = 2.4 Hz), 6.62 (2H, t, J = 8.5 Hz), 5.25 (1H, d, J = 16.7 Hz), 4.50 (2H, m), 4.30 (2H, m), 4.06 (2H, m), 3.64–3.59 (4H, m), 3.53–3.46 (6H, m), 3.67 (4H, m), 3.26 (4H, t, J = 6.8 Hz), 3.01–2.71 (4H, m), 2.39 (1H, dd, J = 16.1, 4.1 Hz), 2.30 (2H, t, J = 7.1 Hz), 2.16 (4H, m), 1.79–1.56 (10H, m), 1.53–1.38 (4H, m). MS (ESI), *m/z*: 800.6 (MH^+), 822.6 (MNa^+).

General Method for the Syntheses of the Antagonist Diketones (17–23) from Their Precursors (24–30). The precursors **24**–**30** (0.1 mmol) were stirred with TFA (0.5 mL) and anisole (0.5 mL) for 16 h at 0 °C. Solvents were removed under vacuum, and the crude products were treated with **1a** (0.11 mmol) in CH_3CN for 2–5 h. It was then worked up using aqueous (10%) citric acid solution and CH_2Cl_2. Solvents were removed under vacuum, and the residues were purified over silica gel (CH_2Cl_2–MeOH, 1:0–3:1), affording pure **17**–**23** in 31–74% yields.

Compound 17. The crude product obtained from the reaction of **24** (73 mg, 0.08 mmol) with TFA (0.5 mL) in the presence of anisole (0.5 mL) in CH_2Cl_2 (2 mL) was reacted with compound **1a** (38 mg, 0.09 mmol) and Et_3N (0.14 mL) in CH_3CN (2 mL) to afford pure **17** (52 mg, 64%). R_f = 0.5 (CH_2Cl_2–MeOH, 4:1). ^{1}H NMR (600 MHz, $CD_3OD/CDCl_3$): δ 7.78 (1H, d, J = 8.3 Hz), 7.61 (1H, m), 7.43 (2H, m), 7.10 (2H, m), 6.89 (2H, s), 6.76 (2H, m), 6.57 (1H, d, J = 8.8 Hz), 6.50 (1H, d, J = 7.0 Hz), 4.29 (1H, m), 4.20 (1H, m), 4.02 (2H, m), 3.98 (1H, m), 3.82 (1H, m), 3.76 (1H, m), 3.70 (2H, m), 3.64 (2H, t, J = 4.4 Hz), 3.52 (2H, t, J = 6.2 Hz), 3.35 (2H, m), 3.23 (2H, t, J = 6.5 Hz), 2.90 (3H, s), 2.91–2.81 (6H, m), 2.64 (6H, s), 2.55 (2H, t, J = 7.4 Hz), 2.35 (2H, t, J = 7.9 Hz), 2.22 (2H, t, J = 7.0 Hz), 2.20 (3H, s), 2.01 (3H, s), 1.93 (2H, m), 1.73 (2H, m). MS (ESI), *m/z*: 987 (MH^+), 1009 (MNa^+), 1025 (MK^+), 985 ($M - H)^-$. HRMS (ESI-TOF high acc) calcd for $C_{51}H_{67}N_6O_{12}S$ 987.4532 (MH^+), found 987.4527.

Compound 18. The crude product obtained from the reaction of **25** (62 mg, 0.08 mmol) with TFA (0.5 mL) in the presence of anisole (0.5 mL) in CH_2Cl_2 (2 mL) was reacted with compound **1a** (38 mg, 0.09 mmol) and Et_3N (0.14 mL) in CH_3CN (2 mL) to afford pure **18** (46 mg, 62%). ^{1}H NMR (500 MHz, $CD_3OD/CDCl_3$): δ 9.00 (1H, s), 8.44 (1H, d, J = 7.3 Hz), 7.69 (1H, d, J = 8.1 Hz), 7.51 (3H, m), 7.05 (2H, d, J = 8.5 Hz), 6.92 (2H, s), 6.85 (1H, s), 6.47 (1H, s), 6.41 (1H, d, J = 8.8 Hz), 6.37 (2H, m), 6.22 (1H, d, J = 6.6 Hz), 5.46 (1H, s), 4.55 (1H, s), 4.11 (1H, s), 3.86 (1H, m), 3.64 (1H, m), 3.53 (1H, s), 3.37 (1H, m), 3.23 (1H, m), 2.90–2.75 (10H, m), 2.65 (6H, s), 2.53 (2H, t, J = 8.1 Hz), 2.32 (2H, m), 2.28 (3H, s), 2.21 (2H, m), 2.03 (3H, s), 1.96 (4H, m), 1.62 (4H, m). MS (ESI), *m/z*: 928 (MH^+), 950 (MNa^+), 926 ($M - H)^-$.

Compound 19. The crude product obtained from the reaction of **26** (93 mg, 0.1 mmol) with TFA (0.5 mL) in the presence of anisole (0.5 mL) in CH_2Cl_2 (2 mL) was reacted with compound **1a** (46 mg, 0.11 mmol) and Et_3N (0.14 mL) in CH_3CN (2 mL) to afford pure **19** (45 mg, 43%). R_f = 0.45 (CH_2Cl_2–MeOH, 4:1). ^{1}H NMR (500 MHz, $CD_3OD/CDCl_3$): δ 7.76 (1H, d, J = 8.1 Hz), 7.67 (1H, t, J = 8.4 Hz), 7.45 (2H, m), 7.11 (2H, m), 6.96 (2H, s), 6.71 (2H, m), 6.65 (1H, d, J = 9.2 Hz), 6.52 (1H, d, J = 7.0 Hz), 4.19 (2H, m), 4.09 (1H, m), 3.76 (1H, dq, J = 9.2, 4.4 Hz), 3.72 (1H, s), 3.67 (1H, t, J = 4.1 Hz), 3.30 (2H, m), 3.20 (2H, t, J = 7.0 Hz), 3.01 (2H, m), 2.99 (3H, s), 2.93 (5H, m), 2.73 (6H, s), 2.62 (2H, t, J = 7.7 Hz), 2.44 (2H, t, J = 7.7 Hz), 2.31 (2H, m), 2.30 (3H, s), 2.25 (2H, t, J = 7.4 Hz), 2.07 (3H, s), 2.04 (4H, m), 1.67 (6H, m), 1.56 (2H, m), 1.38 (2H, m). MS (ESI), *m/z*: 1041 (MH^+), 1063 (MNa^+), 1039 ($M - H)^-$; HRMS (ESI-TOF high acc) calcd for $C_{55}H_{74}N_7O_{11}S$ 1040.5161 (MH^+), found 1040.5164.

Compound 20. The crude product obtained from the reaction of **27** (50 mg, 0.064 mmol) with TFA (0.5 mL) in the presence of anisole (0.5 mL) in CH_2Cl_2 (2 mL) was reacted with compound **1a** (30 mg, 0.07 mmol) and Et_3N (70 μL) in CH_3CN (2 mL) to afford pure **20** (35 mg, 59%). R_f = 0.45 (CH_2Cl_2–MeOH, 4:1). ^{1}H NMR (500 MHz, $CD_3OD/CDCl_3$): δ 7.79 (2H, d, J = 7.4 Hz), 7.62 (2H, d, J = 8.1 Hz), 7.45 (2H, d, J = 7.7 Hz), 7.37 (2H, d, J = 7.0 Hz), 7.32 (2H, m), 7.25 (2H, d, J = 8.1 Hz), 7.12 (2H, d, J = 8.4 Hz), 6.39 (1H, d, J = 7.3 Hz), 6.33 (1H, d, J = 8.4 Hz), 4.65 (1H, dd, J = 9.6, 4.4 Hz), 4.12 (1H, m), 3.90 (1H, m), 3.69 (2H, m), 3.60–3.45 (8H, m), 3.10 (2H, m), 3.04 (2H, t, J = 7.0 Hz), 2.91 (2H, m), 2.88 (3H, s), 2.85 (2H, m), 2.55 (1H, s), 2.42 (1H, m), 2.36 (2H, t, J = 7.3 Hz), 2.22 (2H, t, J = 7.7 Hz), 2.15 (1H, m), 1.98 (3H, s), 1.94 (2H, m), 1.55 (2H, m). MS (ESI), *m/z*: 929 (MH^+), 951 (MNa^+), 927 ($M - H)^-$. HRMS (ESI-TOF high acc) calcd for $C_{48}H_{61}N_6O_{11}S$ 929.4113 (MH^+), found 929.4107.

Compound 21. The crude product obtained from the reaction of **28** (62 mg, 0.08 mmol) with TFA (0.5 mL) in the presence of anisole (0.5 mL) in CH_2Cl_2 (2 mL) was reacted with compound **1a** (38 mg, 0.09 mmol) and Et_3N (0.14 mL) in CH_3CN (2 mL) to afford pure **21** (50 mg, 68%). R_f = 0.8 (CH_2Cl_2–MeOH, 7:3). ^{1}H NMR (600 MHz, $CD_3OD/CDCl_3$): δ 7.73 (2H, d, J = 8.3 Hz), 7.68 (2H, d, J = 8.3 Hz), 7.54 (1H, t, J = 8.3 Hz), 7.43 (2H, m), 7.22 (2H, dd, J = 7.9, 5.3 Hz), 7.10 (2H, m), 6.53 (1H, d, J = 8.8 Hz), 6.47 (1H, d, J = 7.4 Hz), 3.83 (1H, dd, J = 7.4, 4.8 Hz), 3.68 (1H, dd, J = 13.6, 5.3 Hz), 3.63 (1H, dd, J = 13.6, 7.5 Hz), 3.58 (2H, m), 3.53 (4H, m), 3.40 (2H, t, J = 6.6 Hz), 3.36 (2H, t, J = 5.3 Hz), 3.31 (2H, m), 2.99 (2H, m), 2.93 (2H, m), 2.89 (3H, s), 2.85 (2H, t, J = 7.9 Hz), 2.80 (1H, s), 2.64 (2H, t, J = 7.4 Hz), 2.55 (2H, t, J = 7.9 Hz), 2.36 (2H, t, J = 7.4 Hz), 2.26 (2H, t, J = 7.4 Hz), 2.14 (1H, s), 1.99 (3H, s), 1.95 (2H, q, J = 7.0 Hz), 1.79 (2H, m). MS (ESI), *m/z*: 929 (MH^+), 927 ($M - H)^-$. HRMS (ESI-TOF high acc) calcd for $C_{48}H_{61}N_6O_{11}S$ 929.4113 (MH^+), found 929.4120.

Compound 22. The crude product obtained from the reaction of **29** (138 mg, 0.17 mmol) with TFA (1 mL) in the presence of anisole (1 mL) in CH_2Cl_2 (2 mL) was reacted with compound **1a** (78 mg, 0.19 mmol) and Et_3N (0.15 mL) in CH_3CN (2 mL) to afford pure **22** (82 mg, 51%). R_f = 0.3 (CH_2Cl_2–MeOH, 4:1). ^{1}H NMR (500 MHz, $CD_3OD/CDCl_3$): δ 7.66 (2H, d, J = 8.1 Hz), 7.52 (1H, t, J = 7.7 Hz), 7.43 (2H, d, J = 8.4 Hz), 7.21 (2H, d, J = 8.4 Hz), 7.11 (2H, d, J = 8.4 Hz), 6.85 (2H, s), 6.60 (1H, d, J = 8.8 Hz), 6.47 (1H, d, J = 7.0 Hz), 3.74 (1H, m), 3.68 (1H, m), 3.67 (2H, t, J = 5.1 Hz), 3.62 (3H, m), 3.55 (2H, m), 3.47 (4H, m), 3.23 (2H, t, J = 7.0 Hz), 3.00 (2H, m), 2.94 (2H, m), 2.85 (2H, t, J = 7.4 Hz), 2.81 (1H, s), 2.60 (6H, s), 2.55 (2H, t, J = 7.4 Hz), 2.36 (2H, t, J = 7.4 Hz), 2.24 (2H, t, J = 7.3 Hz), 2.17 (3H, s), 1.99 (3H, s), 1.95 (2H, q, J = 7.7 Hz), 1.72 (2H, q, J = 6.3 Hz). MS (ESI), *m/z*: 957 (MH^+), 979 (MNa^+), 995 (MK^+), 955 ($M - H)^-$. HRMS (ESI-TOF high acc) calcd for $C_{50}H_{65}N_6O_{11}S$ 957.4426 (MH^+), found 957.4436.

Compound 23. The crude product obtained from the reaction of **30** (73 mg, 0.08 mmol) with TFA (0.5 mL) in the presence of anisole (0.5 mL) in CH_2Cl_2 (2 mL) was reacted with compound **1a** (37 mg, 0.09 mmol) and Et_3N (80 μL) in CH_3CN (2 mL) to afford pure **23** (60 mg, 74%). R_f = 0.55 (CH_2Cl_2–MeOH, 4:1). ^{1}H NMR (600 MHz, $CD_3OD/CDCl_3$): δ 7.65 (2H, d, J = 8.3 Hz), 7.54 (1H, t, J = 7.9 Hz), 7.44 (2H, m), 7.20 (2H, d, J = 8.3 Hz), 7.12 (2H, m), 6.86 (2H, s), 6.59 (1H, d, J = 8.8 Hz), 6.46 (1H, d, J = 6.6 Hz), 3.73 (1H, dd, J = 7.0, 5.3 Hz), 3.67–3.62 (6H, m), 3.56 (6H, m), 3.48 (2H, t, J = 6.1 Hz), 3.38 (2H, t, J = 7.0 Hz), 3.32 (2H, m), 3.24 (2H, t, J = 7.0 Hz), 2.99 (2H, m), 2.93 (2H, m), 2.85 (2H, t, J = 7.4 Hz), 2.61 (6H, s), 2.56 (2H, t, J = 7.9 Hz), 2.37 (2H, t, J = 7.4 Hz), 2.24 (2H, t, J = 7.4 Hz), 2.18 (3H, s), 2.00 (3H, s), 1.94 (2H, m), 1.88 (2H, m), 1.72 (2H, m). MS (ESI), *m/z*: 1015 (MH^+), 1037 (MNa^+), 1013 ($M - H)^-$. HRMS (ESI-TOF high acc) calcd for $C_{53}H_{71}N_6O_{12}S$ 1015.4845 (MH^+), found 1015.4853.

Acknowledgment. This study was supported by the Skaggs Institute for Chemical Biology.

Supporting Information Available: List of physical data of selected compounds, figures showing the binding modes of compounds **72** and **76**, and grid of the X-ray structure of integrin $\alpha v\beta 3$ used for the AutoDock calculation. This material is available free of charge via the Internet at http://pubs.acs.org.

References

(1) (a) Reichert, J. M. Monoclonal antibodies in the clinic. *Nat. Biotechnol.* **2001**, *19*, 819−822. (b) Brekke, O. H.; Sandlie, I. Therapeutic antibodies for human diseases at the dawn of the twenty-first century. *Nat. Rev. Drug Discovery* **2003**, *2*, 52−62.

(2) Clynes, R. A.; Towers, T. L.; Presta, L. G.; Ravetch, J. V. Inhibitory Fc receptors modulate in vivo cytotoxicity against tumor targets. *Nat. Med.* **2000**, *6*, 443−446.

(3) van Dijk, M. A.; van de Winkel, J. G. J. Human antibodies as next generation therapeutics. *Curr. Opin. Chem. Biol.* **2001**, *5*, 368−374.

(4) (a) Martin, A. B.; Schultz, P. G.Opportunities at the interface of chemistry and biology. *Trends Genet.* **1999**, *15*, M24−M28. (b) Arnold, F. H.; Gliedery, A. Chemistry and biotechnology: a productive union meets new challenges. *Curr. Opin. Biotechnol*. **2003**, *14*, 567−569.

(5) (a) Wagner, J.; Lerner, R. A.; Barbas, C. F., III. Efficient aldolase catalytic antibodies that use the enamine mechanism of natural enzymes. *Science* **1995**, *270*, 1797−1800. (b) Zhong, G.; Lerner, R. A.; Barbas, C. F., III. Broadening the aldolase catalytic antibody repertoire by combining reactive immunization and transition state theory: new enantio- and diastereoselectivities. *Angew. Chem., Int. Ed.* **1999**, *38*, 3738−3741. (c) Karlström, A.; Zhong, G.; Rader, C.; Larsen, N. A.; Heine, A.; Fuller, R.; List, B.; Tanaka, F.; Wilson, I. A.; Barbas, C. F., III; Lerner, R. A. Using antibody catalysis to study the outcome of multiple evolutionary trials of a chemical task. *Proc. Natl. Acad. Sci. U.S.A.* **2000**, *97*, 3878−3883.

(6) Barbas, C. F., III; Heine, A.; Zhong, G.; Hoffmann, T.; Gramatikova, S.; Björnstedt, R.; List, B.; Anderson, J.; Stura, E. A.; Wilson, I. A.; Lerner, R. A. Immune versus natural selection: antibody aldolases with enzymic rates but broader scope. *Science* **1997**, *278*, 2085−2092.

(7) (a) Sinha, S. C.; Barbas, C. F., III; Lerner, R. A.The antibody catalysis route to the total synthesis of epothilones. *Proc. Natl. Acad. Sci. U.S.A.* **1998**, *95*, 14603−14608. (b) List, B.; Shabat, D.; Barbas, C. F.; Lerner, R. A. Enantioselective total synthesis of some brevicomins using aldolase antibody 38C2. *Chem.—Eur. J.* **1998**, *4*, 881−885. (c) Sinha, S. C.; Sun, J.; Miller, G.; Barbas, C. F., III; Lerner, R. A. Sets of Aldolase Antibodies with Antipodal Reactivities. Formal Synthesis of Epothilone E by Large-Scale Antibody-Catalyzed Resolution of Thiazole Aldol. *Org. Lett.* **1999**, *1*, 1623−1626. (d) Sinha, S. C.; Sun, J.; Wartmann, M.; Lerner, R. A. Synthesis of multiple epothilone analogs via antibody catalyzed resolution of thiazole aldol synthons on a multigram scale. Biological consequences of addition of an alkyl group at C-13 of epothilones. *ChemBioChem* **2001**, *2*, 656−665.

(8) (a) Shabat, D.; Rader, C.; List, B.; Lerner, R. A.; Barbas, C. F., III. Multiple event activation of a generic prodrug trigger by antibody catalysis. *Proc. Natl. Acad. Sci. U.S.A.* **1999**, *96*, 6925−6930. (b) Shabat, D.; Lode, H. N.; Pertl, U.; Reisfeld, R. A.; Rader, C.; Lerner, R. A.; Barbas, C. F., III. In vivo activity in a catalytic antibody−prodrug system: antibody catalyzed etoposide prodrug activation for selective chemotherapy. *Proc. Natl. Acad. Sci. U.S.A.* **2001**, *98*, 7528−7533. (c) Sinha, S. C.; Li, L.-S.; Miller, G. P.; Dutta, S.; Rader, C.; Lerner, R. A. Prodrugs of dynemicin analogs for selective chemotherapy mediated by an aldolase catalytic Ab. *Proc. Natl. Acad. Sci. U.S.A.* **2004**, *101*, 3095−3099.

(9) Johnsson, N.; Johnsson, K. A Fusion of Disciplines: Chemical Approaches To Exploit Fusion Proteins for Functional Genomics. *ChemBioChem* **2003**, *4*, 803−810.

(10) Mulford, D. A.; Jurcic, J. G. Antibody-based treatment of acute myeloid leukaemia. *Expert Opin. Biol. Ther.* **2004**, *4*, 95−105.

(11) Rader, C.; Sinha, S. C.; Popkov, M.; Lerner, R. A.; Barbas, C. F., III. Chemically programmed monoclonal antibodies for cancer therapy: Adaptor immunotherapy based on a covalent antibody catalyst. *Proc. Natl. Acad. Sci. U.S.A.* **2003**, *100*, 5396−5400.

(12) Tucker, G. C. αv integrin inhibitors and cancer therapy. *Curr. Opin. Invest. Drugs* **2003**, *4*, 722−731 (and p 1140 for erratum).

(13) For a recent review, see the following: Miller, W. H.; Keenan, R. M.; Willette, R. N.; Lark, M. W. Identification and in vivo efficacy of small-molecule antagonists of integrin αvβ3 (the vitronectin receptor). *Drug Discovery Today* **2000**, *5*, 397−408.

(14) Gutheil, J. C.; Campbell, T. N.; Pierce, P. R.; Watkins, J. D.; Huse, W. D.; Bodkin, D. J.; Cheresh, D. A. *Clin. Cancer Res.* **2000**, *6*, 3056−3061.

(15) Arap, W.; Pasqualini, R.; Ruoslahti, E. Cancer treatment by targeted drug delivery to tumor vasculature in a mouse model. *Science* **1998**, *279*, 377−380.

(16) Kunath, K.; Merdan, T.; Hegener, O.; Häberlein, H.; Kissel, T. Integrin targeting using RGD-PEI conjugates for in vitro gene transfer. *J. Gene Med.* **2003**, *5*, 588−599.

(17) (a) Liu, S.; Cheung, E.; Ziegler, M. C.; Rajopadhye, M.; Edwards, D. S. 90Y and 177Lu Labeling of a DOTA-Conjugated Vitronectin Receptor Antagonist Useful for Tumor Therapy. *Bioconjugate Chem.* **2001**, *12*, 559−568. (b) Janssen, M. L.; Oyen, W. J.; Dijkgraaf, I.; Massuger, L. F.; Frielink, C.; Edwards, D. S.; Rajopadhye, M.; Boonstra, H.; Corstens, F. H.; Boerman, O. C. Tumor targeting with radiolabeled αvβ3 integrin binding peptides in a nude mouse model. *Cancer Res.* **2002**, *62*, 6146−6151.

(18) (a) Pfaff, M.; Tangemann, K.; Muller, B.; Gurrath, M.; Muller, G.; Kessler, H.; Timpl, R.; Engel, J. Selective recognition of cyclic RGD peptides of NMR defined conformation by αIIbβ3, αvβ3, and α5β1 integrins. *J. Biol. Chem.* **1994**, *269*, 20233−20238. (b) Bach, A. C., II; Espina, J. R.; Jackson, S. A.; Stouten, P. F. W.; Duke, J. L.; Mousa, S. A.; Degrado, W. F. Type II′ to Type I β-Turn Swap Changes Specificity for Integrins. *J Am. Chem. Soc.* **1996**, *118*, 293−294. (c) Burgess, K.; Lim, D.; Mousa, S. A. Synthesis and Solution Conformation of cyclo[RGDRGD]: A Cyclic Peptide with Selectivity for the αvβ3 Receptor. *J. Med. Chem.* **1996**, *39*, 4520−4526.

(19) (a) Keenan, R. M.; Miller, W. H.; Kwon, C.; Ali, F. E.; Callahan, J. F.; Calvo, R. R.; Hwang, S.-M.; Kopple, K. D.; Peishoff, C. E.; Samanen, J. M.; Wong, A. S.; Yuan, C.-K.; Huffman, W. F. Discovery of potent nonpeptide vitronectin receptor (α v β 3) antagonists. *J. Med. Chem.* **1997**, *40*, 2289−2292. (b) Miller, W. H.; Alberts, D. P.; Bhatnagar, P. K.; Bondinell, W. E.; Callahan, J. F.; Calvo, R. R.; Cousins, R. D.; Erhard, K. F.; Heerding, D. A.; Keenan, R. M.; Kwon, C.; Manley, P. J.; Newlander, K. A.; Ross, S. T.; Samanen, J. M.; Uzinskas, I. N.; Venslavsky, J. W.; Yuan, C. C.; Haltiwanger, R. C.; Gowen, M.; Hwang, S. M.; James, I. E.; Lark, M. W.; Rieman, D. J.; Stroup, G. B.; Azzarano, L. M.; Salyers, K. L.; Smith, B. R.; Ward, K. W.; Johanson, K. O.; Huffmann, W. F. Discovery of orally active nonpeptide vitronectin receptor antagonists based on a 2-benzazepine Gly-Asp mimetic. *J. Med. Chem.* **2000**, *43*, 22−26.

(20) Duggan, M. E.; Duong, L. T.; Fisher, J. E.; Hamill, T. G.; Hoffman, W. F.; Huff, J. R.; Ihle, N. C.; Leu, C.-T.; Nagy, R. M.; Perkins, J. J.; Rodan, S. B.; Wesolowski, G.; Whitman, D. B.; Zartman, A. E.; Rodan, G. A.; Hartman, G. D. Nonpeptide αvβ3 Antagonists. 1. Transformation of a Potent, Integrin-Selective αIIbβ3 Antagonist into a Potent rvâ3 Antagonist. *J. Med. Chem.* **2000**, *43*, 3736−3745.

(21) (a) Reference 6. (b) Rader, C.; Barbas, C. F., III. Unpublished results.

(22) List, B.; Barbas, C. F., III; Lerner, R. A. Aldol sensors for the rapid generation of tunable fluorescence by antibody catalysis. *Proc. Natl. Acad. Sci. U.S.A.* **1998**, *95*, 15351−15355.

(23) Tanaka, F.; Lerner, R. A.; Barbas, C. F., III. Reconstructing Aldolase Antibodies To Alter Their Substrate Specificity and Turnover. *J. Am. Chem. Soc.* **2000**, *122*, 4835−4836.

(24) Feuston, B. P.; Culberson, J. C.; Duggan, M. E.; Hartman, G. D.; Leu, C.-T.; Rodan, S. B. Binding Model for Nonpeptide Antagonists of αvβ3 Integrin. *J. Med. Chem.* **2002**, *45*, 5640−5648.

(25) (a) Gottschalk, K.-E.; Günther, R.; Kessler, H. A three-state mechanism of integrin activation and signal transduction for integrin αvβ3. *ChemBioChem* **2002**, *3*, 470−473. (b) Marinelli, L.; Lavecchia, A.; Gottschalk, K.-E.; Novellino, E.; Kessler, H. Docking Studies on αvβ3 Integrin Ligands: Pharmacophore Refinement and Implications for Drug Design. *J. Med. Chem.* **2003**, *46*, 4393−4404.

(26) Morris, G. M.; Goodsell, D. S.; Halliday, R. S.; Huey, R.; Hart, W. E.; Belew, R. K.; Olson, A. J. Automated docking using a Lamarckian genetic algorithm and an empirical binding free energy function. *J. Comput. Chem.* **1998**, *19*, 1639−1662.

(27) Xiong, J.-P.; Stehle, T.; Diefenbach, B.; Zhang, R.; Dunker, R.; Scott, D. L.; Joachimiak, A.; Goodman, S. L.; Arnaout, M. A. Crystal Structure of the Extracellular Segment of Integrin αvβ3. *Science* **2001**, *294*, 339−345.

(28) Xiong, J.-P.; Stehle, T.; Zhang, R.; Joachimiak, A.; Frech, M.; Goodman, S. L.; Arnaout, M. A. Crystal Structure of the Extracellular Segment of Integrin αvβ3 in Complex with an Arg-Gly-Asp Ligand. *Science* **2002**, *296*, 151−155.

(29) Smith, J. W.; Cheresh, D. A. The Arg-Gly-Asp binding domain of the vitronectin receptor. Photoaffinity cross-linking implicates amino acid residues 61−203 of the beta subunit. *J. Biol. Chem.* **1988**, *263*, 18726−18731.

(30) Kok, R. J.; Schraa, A. J.; Bos, E. J.; Moorlag, H. E.; Ásgeirsdóttir, S. A.; Everts, M.; Meijer, D. K. F.; Molema, G. Preparation and Functional Evaluation of RGD-Modified Proteins as αvβ3 Integrin Directed Therapeutics. *Bioconjugate Chem.* **2002**, *13*, 128−135.

JM049666K